Communications in Theoretical Physics

Commun. Theor. Phys. **77** (2025) 075403 (9pp) https://doi.org/10.1088/1572-9494/ada87e
CSTR: 32041.14.CTP.ada87e

Gravitational deflection of light in the polar-axis plane of a moving Kerr–Newman black hole

Xuan Wang[1], Wenbin Lin[1,2], Bo Yang[1,3] and Guansheng He[1,3,*]

[1] School of Mathematics and Physics, University of South China, Hengyang 421001, China
[2] School of Physical Science and Technology, Southwest Jiaotong University, Chengdu 610031, China
[3] Purple Mountain Observatory, Chinese Academy of Sciences, Nanjing 210023, China

E-mail: hgs@usc.edu.cn

Received 5 November 2024, revised 16 December 2024
Accepted for publication 10 January 2025
Published 4 April 2025

Abstract

The gravitational deflection of light signals restricted in the polar-axis plane of a moving Kerr–Newman (KN) black hole with a constant velocity along the polar axis is studied within the second post-Minkowskian (PM) approximation. For this purpose, the Lorentz boosting technique is adopted to obtain the exact metric of a moving KN black hole with an arbitrary constant velocity in Kerr–Schild coordinates for the first time. Based on the weak field limit of the exact metric, we then derive the equations of motion of test particles constrained in the polar-axis plane of a moving KN source whose velocity is along the polar axis and collinear with its angular momentum. An iterative technique is utilized subsequently in the calculations of the null deflection angle up to the 2PM order caused by the moving lens, and this deflection angle is found to be spin-independent. Finally, we discuss the influence of the motion of the lens on the gravitational deflection and estimate the possibility of detecting this kinematical effect. Our work might be helpful for future astronomical observations.

Keywords: black holes, exact metric, gravitational lens

(Some figures may appear in colour only in the online journal)

1. Introduction

Gravitational lensing, along with its extensive applications to many fields in astronomy, has developed into one of the most rapidly growing branches of modern astrophysics (see, for instance, [1–37]). Different from much literature with the focus on the gravitational lensing phenomena in a static spherically symmetric or stationary axially symmetric spacetime, the gravitational lensing effects caused by a moving one-body gravitational system or by an N-body system consisting of moving gravitational sources have been the subject of quite a few previous works in the last decades (see, e.g., [38–53] and references therein). For example, a pioneering method on the basis of the influence of the lens' motion on the brightness of an isotropic radiation field was proposed to measure the transversal velocity of a cluster of galaxies [38]. Wucknitz and Sperhake [41] investigated the effects of the radial and transversal motions of a Schwarzschild lens on the gravitational deflection of test particles including photons within the framework of the first post-Minkowskian (PM) approximation. The equatorial bending phenomena of relativistic massive particles and light in the spacetime of a radially moving Kerr–Newman (KN) black hole were also studied [49, 50], with a discussion on the effects of the lens motion on the second-order contributions to the deflection angle. The reasons for the increasing interest in this type of gravitational lensing effect lie mainly in two aspects. On the theoretical side, the so-called velocity effect [41, 42, 54] resulting from the motion of the gravitational source has an influence on the propagation of test particles, and may eventually affect the related observable relativistic effects. It is interesting and necessary to further probe the velocity effects on the lensing

* Author to whom any correspondence should be addressed.

properties for various scenarios in different spacetimes. On the observational aspect, it should be mentioned that those velocity effects for the cases of the lens motions with a relatively large or relativistic velocity may be so evident that they could play a role in the measurements of a part of lensing observables [41, 42, 49]. As is known, high-velocity or hypervelocity celestial bodies (such as stars, neutron stars, or even stellar-mass black holes) are not rare in our universe. For example, the transverse velocity of the pulsar B2224 + 65 is not smaller than 800km/s [55], while the pulsar B1508 + 55 moves with a high transverse velocity $\sim 1083^{+103}_{-90}$ km/s [56]. When such a high-velocity celestial body serves as the gravitational lens, a full consideration of the lens motion effects on both the first-order contributions and the higher-order contributions to the lensing properties (e.g., the differential time delay of the primary and secondary images of the source) is necessary for future high-accuracy astronomical observations, as discussed in [49]. Additionally, it is known that rapid improvement of high-accuracy astronomical instruments and techniques has been achieved in the past decades. Current and forthcoming surveys with multi-wavelength observations are working towards an astrometric precision of 1 ~ 10 microarcseconds (μas) or better [57–71]. For example, the Square Kilometre Array (SKA) [70, 72] and other next-generation radio observatories (see [67, 68], and references therein) aim at an angular accuracy of about 1μas. With the steady progress made in high-accuracy position, time, and angular measurements and the increase in the multi-messenger synergic observations (see, e.g., [73–77]), further consideration of gravitational lensing due to a moving lens becomes more and more meaningful and thus deserves our efforts.

However, to the best of our knowledge, most of the related works were devoted to the discussion of the velocity effects on the propagation of test particles constrained in the equatorial plane of the lens and the full influence of the gravitational source's motion on the lensing properties of lightlike or timelike signals traveling off the lens' equatorial plane [78–81] has not been considered to date. As a first step of a full theoretical treatment of it, here we mainly focus on probing the velocity effects on the gravitational deflection of light in the polar-axis plane of a moving KN lens. Additionally, the handling of this issue fundamentally requires the knowledge of the gravitational field of the background spacetime. Hence, the achievement of the metric of a moving KN black hole naturally becomes another part of our concern.

In the present paper, we utilize the Lorentz boosting technique [41, 54, 82] to derive the Kerr–Schild form of the exact metric of a constantly moving KN black hole, which is regarded as an extension of a series of exact metrics of moving black holes [53, 83, 84]. Our attention is then concentrated on the investigation of the gravitational deflection effect of light restricted in the polar-axis plane of a moving KN black hole with its constant velocity along the polar axis within the 2PM approximation. It is interesting to find that this deflection angle is spin-independent. Moreover, the effect of the lens' motion on the gravitational deflection of light is discussed and the possibility of detecting the resulting velocity effect is evaluated. Our discussions are limited to the weak-field, small-angle, and thin-lens approximation.

The outline of this paper is as follows. We derive the Kerr–Schild form of the exact metric of a constantly moving KN black hole in section 2. As an application of the weak field limit of this solution, the null gravitational deflection in the polar-axis plane of a moving KN black hole with a constant velocity along the polar axis is probed in the 2PM approximation in section 3, accompanied by a discussion of the velocity effect on the deflection angle. Section 4 subsequently presents a summary. Throughout this paper, the metric signature (− , + , + , +) and the geometrized units in which $G = c = 1$ are adopted, Greek indices run over 0, 1, 2, and 3, and Latin indices run over 1, 2, and 3.

2. The metric of a constantly moving KN black hole

Let $\boldsymbol{e}_i (i = 1,\ 2,\ 3)$ denote the orthonormal basis of a three-dimensional Cartesian coordinate system. $x^\nu = (t,\ x_1,\ x_2,\ x_3)$ and $X^\nu \equiv (T, X_1, X_2, X_3) = (T, \boldsymbol{X})$ stand for the rest Kerr–Schild coordinate frame of the observer of the background and the comoving Kerr–Schild coordinate frame of the gravitational source, respectively. The gravitational field outside a constantly rotating and charged black hole is described by the KN metric, which reads in the comoving Kerr–Schild frame [85–88]:

$$\begin{aligned} \mathrm{d}s^2 = &-\mathrm{d}T^2 + \mathrm{d}X_1^2 + \mathrm{d}X_2^2 + \mathrm{d}X_3^2 + \frac{(2MR - Q^2)R^2}{R^4 + a^2 Z^2} \\ &\times \left[\mathrm{d}T + \frac{X_3 \mathrm{d}X_3}{R} + \frac{R(X_1 \mathrm{d}X_1 + X_2 \mathrm{d}X_2) - a(X_1 \mathrm{d}X_2 - X_2 \mathrm{d}X_1)}{R^2 + a^2}\right]^2, \end{aligned} \tag{1}$$

where R is defined by the relation $\frac{X_1^2 + X_2^2}{R^2 + a^2} + \frac{X_3^2}{R^2} = 1$, and M, Q, and $a (\equiv |\boldsymbol{J}|/M)$ represent the rest mass, electric charge, and angular momentum per unit mass of the KN black hole, respectively, with $\boldsymbol{J} \equiv J\boldsymbol{e}_3$ along the polar axis.

Based on the Lorentz boosting technique [41] and equation (1), the external gravitational field of a moving KN black hole can be obtained. We know that the Lorentz transformation between the observer's rest frame, in which a KN black hole moves with an arbitrary constant velocity $\boldsymbol{v} = v_1\boldsymbol{e}_1 + v_2\boldsymbol{e}_2 + v_3\boldsymbol{e}_3$, and the comoving frame of the black hole has the form

$$X^\rho = \Lambda^\rho_\sigma x^\sigma, \tag{2}$$

where

$$\Lambda^0_0 = \gamma, \tag{3}$$

$$\Lambda^i_0 = \Lambda^0_i = -v_i\gamma, \tag{4}$$

$$\Lambda^i_j = \delta_{ij} + \frac{(\gamma - 1)v_i v_j}{v^2}. \tag{5}$$

Here, $v \equiv |\boldsymbol{v}| = \sqrt{v_1^2 + v_2^2 + v_3^2}$, and $\gamma \equiv (1 - v^2)^{-\frac{1}{2}}$ denotes the Lorentz factor. By applying the definition of the covariant metric tensor, the exact metric of the moving KN black hole can be achieved in the observer's rest Kerr–Schild frame $(t,\ x_1,\ x_2,\ x_3)$ as follows:

$$g_{00} = -1 + \frac{\gamma^2(2MR - Q^2)R^2}{R^4 + a^2X_3^2} \times \left[1 - \frac{v_1(RX_1 + aX_2)}{R^2 + a^2} - \frac{v_2(RX_2 - aX_1)}{R^2 + a^2} - \frac{v_3X_3}{R}\right]^2, \quad (6)$$

$$g_{0i} = \frac{\gamma(2MR - Q^2)R^2}{R^4 + a^2X_3^2} \times \left[1 - \frac{v_1(RX_1 + aX_2)}{R^2 + a^2} - \frac{v_2(RX_2 - aX_1)}{R^2 + a^2} - \frac{v_3X_3}{R}\right] \times \{\frac{(RX_1 + aX_2)\delta_{1i}}{R^2 + a^2} + \frac{(RX_2 - aX_1)\delta_{2i}}{R^2 + a^2} + \frac{X_3\delta_{3i}}{R} - v_i\gamma + \frac{v_i(\gamma - 1)}{v^2} \times \left[\frac{v_1(RX_1 + aX_2)}{R^2 + a^2} + \frac{v_2(RX_2 - aX_1)}{R^2 + a^2} + \frac{v_3X_3}{R}\right]\}, \quad (7)$$

$$g_{ij} = \delta_{ij} + \frac{(2MR - Q^2)R^2}{R^4 + a^2X_3^2}\left\{\frac{(RX_1 + aX_2)\delta_{1i}}{R^2 + a^2} + \frac{(RX_2 - aX_1)\delta_{2i}}{R^2 + a^2} + \frac{X_3\delta_{3i}}{R} - v_i\gamma + \frac{v_i(\gamma - 1)}{v^2} \times \left[\frac{v_1(RX_1 + aX_2)}{R^2 + a^2} + \frac{v_2(RX_2 - aX_1)}{R^2 + a^2} + \frac{v_3X_3}{R}\right]\right\} \times \left\{\frac{(RX_1 + aX_2)\delta_{1j}}{R^2 + a^2} + \frac{(RX_2 - aX_1)\delta_{2j}}{R^2 + a^2} + \frac{X_3\delta_{3j}}{R} - v_j\gamma + \frac{v_j(\gamma - 1)}{v^2} \times \left[\frac{v_1(RX_1 + aX_2)}{R^2 + a^2} + \frac{v_2(RX_2 - aX_1)}{R^2 + a^2} + \frac{v_3X_3}{R}\right]\right\}, \quad (8)$$

where δ_{ij} denotes the Kronecker delta. We can see that equations (6) - (8) for the case of no rotation of the black hole reduce to the Kerr–Schild form of the exact metric of a constantly moving Reissner–Nordström source

$$g_{00} = -1 + \frac{\gamma^2(2MR - Q^2)}{R^2}\left(1 - \frac{\boldsymbol{v}\cdot\boldsymbol{X}}{R}\right)^2, \quad (9)$$

$$g_{0i} = \frac{\gamma(2MR - Q^2)}{R^2}\left(1 - \frac{\boldsymbol{v}\cdot\boldsymbol{X}}{R}\right) \times \left[\frac{X_i}{R} - v_i\gamma + \frac{v_i(\gamma - 1)(\boldsymbol{v}\cdot\boldsymbol{X})}{v^2R}\right], \quad (10)$$

$$g_{ij} = \delta_{ij} + \frac{2MR - Q^2}{R^2}\left[\frac{X_i}{R} - v_i\gamma + \frac{v_i(\gamma - 1)(\boldsymbol{v}\cdot\boldsymbol{X})}{v^2R}\right] \times \left[\frac{X_j}{R} - v_j\gamma + \frac{v_j(\gamma - 1)(\boldsymbol{v}\cdot\boldsymbol{X})}{v^2R}\right], \quad (11)$$

where the distance between the gravitational source and the field point is reduced to $R = |\boldsymbol{X}| = \sqrt{X_1^2 + X_2^2 + X_3^2}$.

3. Weak-field deflection in the polar-axis plane of a KN black hole moving along the polar axis

In this section, we first derive the weak-field geodesic equations of test particles constrained in the polar-axis plane ($x_1 = \partial/\partial x_1 = 0$) of a moving KN black hole whose velocity is assumed to be along the polar axis (i.e., $\boldsymbol{v} = v_3\boldsymbol{e}_3$) for simplicity, and then calculate the null gravitational deflection up to the 2PM order in the polar-axis plane of this moving lens. A brief discussion of the velocity effect on the deflection angle is given subsequently.

3.1. The metric of the moving KN source up to the 2PM order

In order to calculate the polar-axis-plane equations of motion in the gravitational field of the moving lens up to the 2PM order, we need the weak-field form of the spacetime metric, which can be expanded from equations (6)–(8) in the form

$$g_{00} = -1 + \frac{\gamma_P^2(2MR - Q^2)}{R^2}\left(1 - \frac{v_3X_3}{R}\right)^2 + \mathcal{O}(M^3), \quad (12)$$

$$g_{0i} = \gamma_P\left(1 - \frac{v_3X_3}{R}\right)\left\{\frac{2MR - Q^2}{R^2}\left[\frac{X_i}{R} + \left(\frac{(\gamma_P - 1)X_3}{R} - v_3\gamma_P\right)\delta_{3i}\right] + \frac{2aMX_2\delta_{1i}}{R^3}\right\} + \mathcal{O}(M^3), \quad (13)$$

$$g_{ij} = \delta_{ij} + \frac{2MR - Q^2}{R^2}\left[\frac{X_i}{R} + \left(\frac{(\gamma_P - 1)X_3}{R} - v_3\gamma_P\right)\delta_{3i}\right] \times \left[\frac{X_j}{R} + \left(\frac{(\gamma_P - 1)X_3}{R} - v_3\gamma_P\right)\delta_{3j}\right] + \frac{2aMX_2}{R^3}\left\{\left[\frac{X_j}{R} + \left(\frac{(\gamma_P - 1)X_3}{R} - v_3\gamma_P\right)\delta_{3j}\right]\delta_{1i} + \left[\frac{X_i}{R} + \left(\frac{(\gamma_P - 1)X_3}{R} - v_3\gamma_P\right)\delta_{3i}\right]\delta_{1j}\right\} + \mathcal{O}(M^3), \quad (14)$$

where $\gamma_P = (1 - v_3^2)^{-\frac{1}{2}}$ and $R = \sqrt{X_2^2 + X_3^2}$, with a reduced Lorentz transformation given by

$$X_2 = x_2,\ X_3 = \gamma_P(x_3 - v_3t),\ T = \gamma_P(t - v_3x_3). \quad (15)$$

3.2. Equations of motion in the polar-axis plane of the moving black hole

Based on equations (12)—(14), we can get the 2PM geodesic equations of light constrained in the polar-axis plane of the moving KN lens

$$\begin{aligned}0 = {} & \ddot{t} - \gamma_P^3\left\{\frac{v_3M[(R - v_3X_3)X_3 + 2v_3x_2^2]}{R^5} - \frac{2M^2(R - v_3X_3)^2}{R^6} - \frac{v_3Q^2[(R - v_3X_3)X_3 + v_3x_2^2]}{R^6}\right\} \times (R - v_3X_3)\dot{t}^2 + \gamma_P^3\{\frac{M[2(X_3^2 - x_2^2)R - v_3(3X_3^2 - v_3^2R^2)X_3]}{R^5} \\ & + \frac{2M^2(X_3 - v_3R)^2(R - v_3X_3)}{R^6} + \frac{Q^2[v_3\gamma_P^{-2}R^2X_3 - 2(R - v_3X_3)X_3^2 + R\,x_2^2]}{R^6}\}\,\dot{x}_3^2 \\ & + \frac{2\gamma_P^2M(R - 3v_3X_3)(R - v_3X_3)x_2\,\dot{t}\,\dot{x}_2}{R^5} \\ & + 2\gamma_P^3\{\frac{M[(R - v_3X_3)X_3 + 2v_3x_2^2]}{R^5} + \frac{2M^2(X_3 - v_3R)(R - v_3X_3)}{R^6} - \frac{Q^2[(R - v_3X_3)X_3 + v_3x_2^2]}{R^6}\} \\ & \times (R - v_3X_3)\dot{t}\dot{x}_3 + \frac{2\gamma_P^2M[4(R - v_3X_3)X_3 - v_3x_2^2]x_2\dot{x}_2\dot{x}_3}{R^5} \\ & + \mathcal{O}(M^3),\end{aligned} \quad (16)$$

$$
\begin{aligned}
0 = \ddot{x}_2 &+ \{\frac{M[X_3^2+(3\gamma_P^2-2)x_2^2]}{R^5} - \frac{2\gamma_P^2M^2(R-v_3X_3)^2}{R^6} \\
&- \frac{Q^2[X_3^2+(2\gamma_P^2-1)x_2^2]}{R^6}\}x_2\dot{t}^2 \\
&- \left[\frac{M(R^2-3\gamma_P^2x_2^2)}{R^5} + \frac{2\gamma_P^2M^2(X_3-v_3R)^2}{R^6} - \frac{Q^2(R^2-2\gamma_P^2x_2^2)}{R^6}\right] \\
&\times x_2\dot{x}_3^2 + \frac{6v_3\gamma_PMX_3x_2^2\,\dot{t}\,\dot{x}_2}{R^5} - 2\gamma_P^2 \\
&\times \left[\frac{3\,v_3Mx_2^2}{R^5} + \frac{2M^2(X_3-v_3R)(R-v_3X_3)}{R^6} - \frac{2\,v_3\,Q^2x_2^2}{R^6}\right] \\
&\times x_2\,\dot{t}\,\dot{x}_3 - \frac{6\gamma_PMX_3\,x_2^2\,\dot{x}_2\,\dot{x}_3}{R^5} + \mathcal{O}(M^3),
\end{aligned}
\tag{17}
$$

$$
\begin{aligned}
0 = \ddot{x}_3 &+ \gamma_P^3\{\frac{M[\,(R^2-3v_3^2X_3^2)X_3+2v_3^3(X_3^2-x_2^2)R\,]}{R^5} \\
&- \frac{2M^2(X_3-v_3R)(R-v_3X_3)^2}{R^6} \\
&- \frac{Q^2[\gamma_P^{-2}R^2X_3-2v_3^2(X_3-v_3R)X_3^2-v_3^3Rx_2^2]}{R^6}\} \\
&\times \dot{t}^2 - \gamma_P^3(X_3-v_3R)\{\frac{M[(X_3-v_3R)X_3-2x_2^2]}{R^5} \\
&+ \frac{2M^2(X_3-v_3R)^2}{R^6} - \frac{Q^2[(X_3-v_3R)X_3-x_2^2]}{R^6}\}\dot{x}_3^2 \\
&+ \frac{2\,v_3\gamma_P^2M[4(X_3-v_3R)X_3+x_2^2]x_2\dot{t}\dot{x}_2}{R^5} \\
&+ 2\gamma_P^3(X_3-v_3R)\{\frac{v_3M[(X_3-v_3R)X_3-2x_2^2]}{R^5} \\
&- \frac{2M^2(X_3-v_3R)(R-v_3X_3)}{R^6} - \frac{v_3\,Q^2}{R^6} \\
&\times [(X_3-v_3R)X_3-x_2^2]\}\,\dot{t}\dot{x}_3 \\
&- \frac{2\gamma_P^2M(3X_3-v_3R)(X_3-v_3R)x_2\,\dot{x}_2\dot{x}_3}{R^5} + \mathcal{O}(M^3),
\end{aligned}
\tag{18}
$$

where a dot denotes the derivative with respect to the affine parameter ξ which traces the trajectory of a light ray [41, 89], and we have neglected the third- and higher-order terms such as the ones containing the factor $M\dot{x}_2^2$ or $M^2\dot{x}_2$, since $\dot{x}_2$ is regarded to be of the order of M/b_P [90] in which b_P denotes the impact parameter. Interestingly, it is found that all of the spin-dependent contributions have vanished in equations (16)–(18). Moreover, it should be mentioned that due to the frame dragging effect caused by the lens' rotation, the trajectory of light propagating in the polar-axis plane of the moving black hole, indicated by equations (16)–(18), is regarded as the projection of a three-dimensional path of light.

3.3. The 2PM gravitational deflection of light by the moving lens

Now we consider the gravitational deflection up to the 2PM order of light constrained in the polar-axis plane of the moving KN black hole with a velocity $\boldsymbol{v} = v_3\boldsymbol{e}_3$ along the polar axis. Figure 1 presents the corresponding geometrical diagram for light propagating from the source A to the receiver B in the polar-axis plane of the moving KN lens.

We then calculate the polar-axis-plane gravitational deflection of light up to the 2PM order iteratively via the approach developed in [41, 50]. A gravitational bending angle of a test particle is the difference in the propagation directions of the test particle and is defined in our scenario by [50]

$$
\begin{aligned}
\alpha_P &\equiv \arctan\frac{\mathrm{d}x_2}{\mathrm{d}x_3}\Big|_{\xi\to-\infty}^{\xi\to+\infty} \\
&= \arctan\frac{\dot{x}_2}{\dot{x}_3}\Big|_{x_3\to-\infty}^{x_3\to+\infty} = \frac{\dot{x}_2}{\dot{x}_3}\Big|_A^B + \mathcal{O}(M^3),
\end{aligned}
\tag{19}
$$

where the third- and higher-order contributions to the deflection effect have been omitted in the last equality.

By using the boundary conditions $\dot{t}|_{\xi\to-\infty} = \dot{t}|_{x_3\to-\infty} = 1$, $\dot{x}_2|_{\xi\to-\infty} = \dot{x}_2|_{x_3\to-\infty} = 0$, and $\dot{x}_3|_{\xi\to-\infty} = \dot{x}_3|_{x_3\to-\infty} = 1$ and assuming that ξ has the dimension of length [41], we get the following zeroth-order expressions from equations (16)–(18):

$$\dot{t} = 1 + \mathcal{O}(M), \tag{20}$$

$$\dot{x}_2 = 0 + \mathcal{O}(M), \tag{21}$$

$$\dot{x}_3 = 1 + \mathcal{O}(M). \tag{22}$$

With the help of equation (15) and the boundary condition $x_2|_{\xi\to-\infty} = x_2|_{x_3\to-\infty} = -b_P$, equations (20)–(22) further imply the analytical forms of the coordinate x_2 and the parameter and coordinate transformations up to the 0PM order

$$x_2 = -b_P + \mathcal{O}(M), \tag{23}$$

$$\mathrm{d}\xi = [1 + \mathcal{O}(M)]\mathrm{d}x_3, \tag{24}$$

$$\mathrm{d}x_3 = [(1-v_3)^{-1}\gamma_P^{-1} + \mathcal{O}(M)]\mathrm{d}X_3. \tag{25}$$

Now we substitute equations (20)–(25) into equations (16)–(18) and thus obtain

$$
\begin{aligned}
\dot{t} = 1 &+ \frac{M[2(X_3^2+b_P^2)+2X_3\sqrt{X_3^2+b_P^2}+v_3b_P^2]}{(1+v_3)(X_3^2+b_P^2)^{\frac{3}{2}}} \\
&+ \mathcal{O}(M^2),
\end{aligned}
\tag{26}
$$

$$\dot{x}_2 = \frac{(1-v_3)\gamma_PMX_3(2X_3^2+3b_P^2)}{b_P(X_3^2+b_P^2)^{\frac{3}{2}}} + \mathcal{O}(M^2), \tag{27}$$

$$
\begin{aligned}
\dot{x}_3 = 1 &+ \frac{M[b_P^2+2v_3\sqrt{X_3^2+b_P^2}(\sqrt{X_3^2+b_P^2}+X_3)]}{(1+v_3)(X_3^2+b_P^2)^{\frac{3}{2}}} \\
&+ \mathcal{O}(M^2).
\end{aligned}
\tag{28}
$$

Additionally, integrating equation (27) over ξ and using equations (23)–(25), we can get the 1PM expression of x_2

$$x_2 = -b_P\left[1 - \frac{M(2X_3^2+b_P^2)}{b_P^2\sqrt{X_3^2+b_P^2}}\right] + \mathcal{O}(M^2). \tag{29}$$

The analytical form of the parameter transformation up to the 1PM order can be obtained directly from equation (28) as

$$
\begin{aligned}
\mathrm{d}\xi = \Big\{1 &- \frac{M[b_P^2+2v_3\sqrt{X_3^2+b_P^2}(\sqrt{X_3^2+b_P^2}+X_3)]}{(1+v_3)(X_3^2+b_P^2)^{\frac{3}{2}}} \\
&+ \mathcal{O}(M^2)\}\,\mathrm{d}x_3.
\end{aligned}
\tag{30}
$$

Simultaneously, the association of equations (26) and (28) with the reduced Lorentz transformation shown in equation (15) implies the 1PM expression of the coordinate transformation:

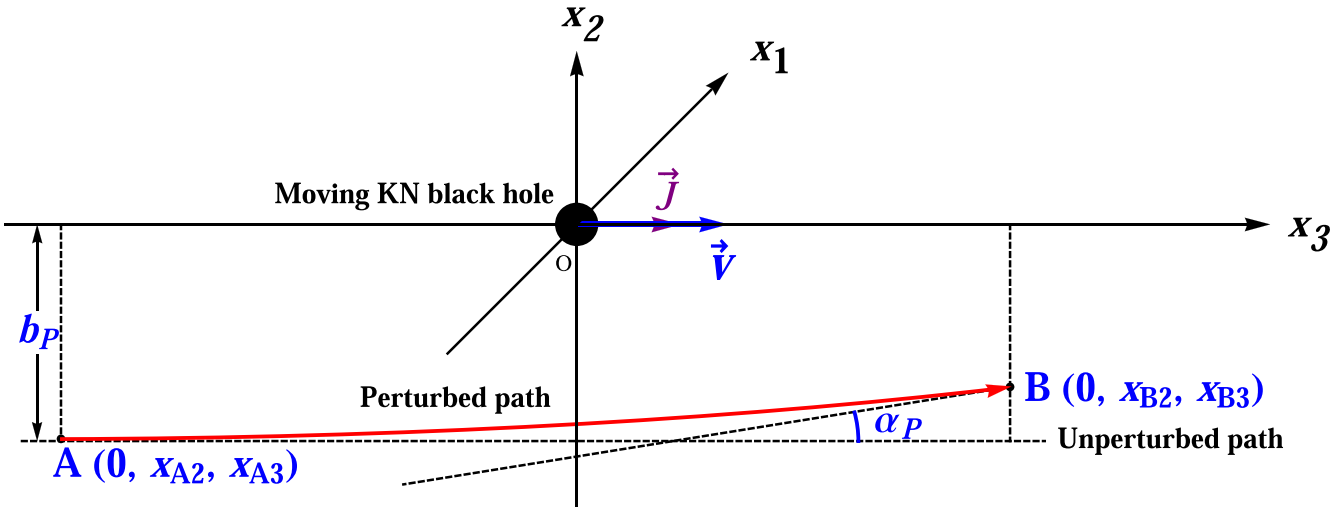

Figure 1. Geometrical diagram for the propagation of light, which is emitted by the source A and received by the detector B, constrained in the polar-axis plane of a moving KN lens whose angular momentum $\boldsymbol{J}$ and constant velocity $\boldsymbol{v}$ are along the x_3-axis. The red line stands for the propagation trajectory of light traveling from $x_3 \to -\infty$ with an initial velocity $\boldsymbol{w} = \boldsymbol{e}_3$, b_P is the impact parameter, and α_P denotes the deflection angle. The coordinates of the source and detector of light in the background's rest frame are denoted, respectively, by $(0, x_{A2}, x_{A3})$ and $(0, x_{B2}, x_{B3})$, with $x_{A2} \approx -b_P$, $x_{A3} \ll -b_P$, and $x_{B3} \gg b_P$. Their coordinates in the comoving frame are denoted by $(0, X_{A2}, X_{A3})$ and $(0, X_{B2}, X_{B3})$, respectively. The gravitational bending effect is exaggerated greatly to distinguish the perturbed propagating path (the red line) from the unperturbed one (the dashed horizontal line).

$$\mathrm{d}x_3 = \frac{1}{(1-v_3)\gamma_P} \times \left[1 + \frac{v_3 M(\sqrt{X_3^2+b_P^2}+X_3)^2}{(1+v_3)(X_3^2+b_P^2)^{\frac{3}{2}}} + \mathcal{O}(M^2)\right]\mathrm{d}X_3. \tag{31}$$

We next substitute equations (26)-(29) into the integration of equation (17) over ξ, adopt the 1PM parameter and coordinate transformations given in equations (30)-(31), and obtain up to the 2PM order

$$\dot{x}_2 = (1-v_3)\gamma_P\left\{\frac{M(2X_3^2+3b_P^2)X_3}{(X_3^2+b_P^2)^{\frac{3}{2}}b_P} - \frac{Q^2\left[5X_3b_P^3+3X_3^3b_P+3(X_3^2+b_P^2)^2\arctan\frac{X_3}{b_P}\right]}{4(X_3^2+b_P^2)^2b_P^2} + \frac{3M^2\left[5X_3^5b_P+16X_3^3b_P^3+7X_3b_P^5+5(X_3^2+b_P^2)^3\arctan\frac{X_3}{b_P}\right]}{4(X_3^2+b_P^2)^3b_P^2}\right\} + \mathcal{O}(M^3). \tag{32}$$

Eventually, the substitution of equations (28) and (32) into equation (19), along with the conditions $X_{A3} \ll -b_P$ ($\approx X_{A2}$) and $X_{B3} \gg b_P$ in the comoving Kerr–Schild frame, gives the gravitational deflection angle up to the 2PM order for light propagating from the source A to the receiver B in the polar-axis plane of the moving KN lens, which is expressed in the observer's rest Kerr–Schild frame as

$$\alpha_P = (1-v_3)\gamma_P\left(\frac{4M}{b_P} + \frac{15\pi M^2}{4b_P^2} - \frac{3\pi Q^2}{4b_P^2}\right) + \mathcal{O}(M^3). \tag{33}$$

With respect to equation (33), three aspects should be mentioned. The first one is that the polar-axis-plane bending angle shown in equation (33) is independent of the rotation or angular momentum of the moving KN black hole. Secondly, we find that for the case of no translational motion of the lens ($v_3 = 0$), equation (33) matches well with the result of the null gravitational deflection in the polar-axis plane of a stationary KN lens derived in harmonic coordinates (see Appendix for details). Finally, the deflection angle α_P is plotted as the function of the impact parameter b_P and the polar-axis velocity v_3 of the moving KN black hole in color-indexed form on the left of figure 2, and its values for a typical weak field $M/b_P = 1.0 \times 10^{-5}$ are shown in table 1.

3.4. Discussion of the velocity effect

As an example of potential astrophysical applications of the result, we assume that the moving KN black hole resulting from the merger of two unequal-mass black holes, receives a recoil (or a 'kick') because of the asymmetric loss of linear momentum in the gravitational radiation [91], and thus obtains a constant kick velocity $\boldsymbol{v}_3 (= v_3\boldsymbol{e}_3)$ along the polar axis. To discuss the influence of the lens' motion on the polar-axis-plane deflection more conveniently, we define a pure velocity-induced effect $\Delta\alpha_P \equiv \alpha_P - \alpha_P|_{v_3=0}$, which means the deviation of α_P from the polar-axis-plane deflection angle due to a stationary KN source and is shown as the color-indexed function of b_P and the polar-axis kick velocity v_3 in figure 2.

It indicates from figure 2, as well as table 1 which contains some values of $\Delta\alpha_P$, that the velocity effect on the polar-axis-plane deflection angle increases monotonously with the decrease of the kick velocity from a positive ultra-

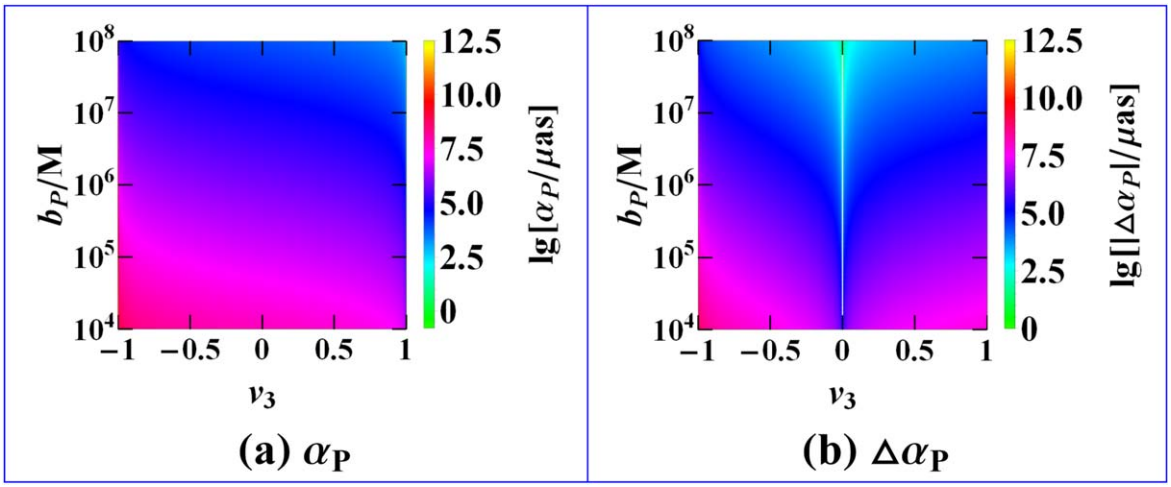

Figure 2. The polar-axis-plane deflection angle α_P and the velocity effect $\Delta\alpha_P$ plotted for various v_3 and b_P in color-indexed form. Here a weak electrical charge $Q = 0.01M$ of the moving lens is assumed.

Table 1. The values (in units of μas) of α_P and $\Delta\alpha_P$ for different polar-axis velocity v_3. A typical weak field $M/b_P = 1.0 \times 10^{-5}$ and $Q = 0.01M$ are assumed.

v_3\Observables	α_P	$\Delta\alpha_P$
0.99	5.85×10^5	-7.67×10^6
0.9	1.89×10^6	-6.36×10^6
0.1	7.46×10^6	-7.88×10^5
0.001	8.24×10^6	-8.25×10^3
0.00001	8.25×10^6	−82.51
0.0000001	8.25×10^6	−0.83
−0.0000001	8.25×10^6	0.83
−0.00001	8.25×10^6	82.51
−0.001	8.26×10^6	8.25×10^3
−0.1	9.12×10^6	8.71×10^5
−0.9	3.60×10^7	2.77×10^7
−0.99	1.16×10^8	1.08×10^8

relativistic value (i.e., $v_3 \to 1$) to a negative ultra-relativistic one (i.e., $v_3 \to -1$). With respect to the detectability of $\Delta\alpha_P$, we find that its absolute values are so large that it is still possible to measure this velocity effect in near future (or even current) resolution when the lens takes a nonrelativistic motion at a low kick velocity. For example, if the galactic supermassive black hole (i.e., Sgr A*) with a rest mass $M = 2.0 \times 10^{-10}$ kpc [92, 93] is assumed to be the lens and moves at a small kick velocity $v_3 = 0.0001$ (~ 30km/s), then the velocity effect $|\Delta\alpha_P|$ is about 288.9μas when we suppose the impact parameter b_P to take a special value 5.74×10^{-5} kpc [94] of the Einstein radius of Sgr A*. It is noticed that this value of $\Delta\alpha_P$ exceeds evidently the current multiwavelength astrometric precision (at the tens of μas level or better [69, 95]), and is much larger than the intended angular accuracy of next-generation radio observatories (such as the SKA [70, 72]).

4. Summary

In this work, we have focused on the investigation of the gravitational deflection effect up to the 2PM order for light constrained in the polar-axis plane of a moving KN black hole with a constant velocity along the polar axis. By means of the Lorentz boosting technique in Kerr–Schild coordinates, we have obtained the exact metric of a moving KN black hole with an arbitrary constant velocity for the first time. The weak-field form of the resulting metric is then applied to the calculations of the dynamics of light, on the basis of which the null polar-axis-plane deflection angle induced by the moving KN lens whose velocity is along the polar axis has been derived iteratively. It is interesting to find that the polar-axis-plane bending angle is independent of the intrinsic angular momentum of the rotating lens. The velocity-induced effect due to the lens' translational motion on the gravitational deflection has also been discussed. With the consideration that the study of the propagation of light signals in time-dependent gravitational fields is important for modern relativistic astrophysics and fundamental astrometry, it should be expected that the results presented in this work might be helpful for future astronomical observations.

Acknowledgments

This work was supported in part by the National Natural Science Foundation of China (grant Nos. 11973025, 12205139, 12303079, 12475057, and 12481540180) and the Natural Science Foundation of Hunan Province (grant No. 2022JJ40347). G.H. would like to thank Yi Xie for an enlightening discussion.

Appendix Null gravitational deflection restricted in the polar-axis plane of a stationary KN black hole in harmonic coordinates

The weak-field metric of a stationary KN black hole can be written in harmonic coordinates $x_H^\mu \equiv (t,\ x_H,\ y_H,\ z_H) = (t,\ \boldsymbol{x}_H)$ as follows:

$$g_{00} = -1 + \frac{2M}{r_H} - \frac{2M^2}{r_H^2} - \frac{Q^2}{r_H^2} + \mathcal{O}(M^3), \tag{A.1}$$

$$g_{0i} = \zeta_i + \mathcal{O}(M^3), \tag{A.2}$$

$$g_{ij} = \left(1 + \frac{M}{r_H}\right)^2 \delta_{ij} + \frac{M^2 - Q^2}{r_H^2}\frac{x_H^i x_H^j}{r_H^2} + \mathcal{O}(M^3), \tag{A.3}$$

where M, Q, and δ_{ij} have been defined above, r_H is related to x_H, y_H, and z_H by $\frac{x_H^2+y_H^2}{r_H^2+a^2} + \frac{z_H^2}{r_H^2} = 1$, and $\boldsymbol{\zeta} \equiv \frac{2a\boldsymbol{M}}{r_H^3}$ $(\boldsymbol{x}_H \times \boldsymbol{e_3}) = (\zeta_1,\ \zeta_2,\ 0)$. Combining equations (A.1)-(A.3) and the geodesic equations $\frac{\mathrm{d}^2x^\mu}{\mathrm{d}\xi^2} + \Gamma^\mu_{\nu\lambda}\frac{\mathrm{d}x^\nu}{\mathrm{d}\xi}\frac{\mathrm{d}x^\lambda}{\mathrm{d}\xi} = 0$ where $\Gamma^\mu_{\nu\lambda}$ is the Christoffel symbol, we get the 2PM equations of motion for light constrained in the polar-axis plane ($x_H = \partial/\partial x_H = 0$) of the KN source

$$0 = \ddot{t} + \frac{2My_H\dot{t}\dot{y}_H}{r_H^3} + \frac{2(Mr_H - Q^2)z_H\dot{t}\dot{z}_H}{r_H^4} + \mathcal{O}(M^3), \tag{A.4}$$

$$\begin{aligned} 0 = \ddot{y}_H &+ \frac{(Mr_H - 4M^2 - Q^2)y_H\dot{t}^2}{r_H^4} \\ &+ \frac{[Mr_H^3 - 2M^2z_H^2 + Q^2(z_H^2 - y_H^2)]y_H\dot{z}_H^2}{r_H^6} \\ &- \frac{2Mz_H\dot{y}_H\dot{z}_H}{r_H^3} + \mathcal{O}(M^3), \end{aligned} \tag{A.5}$$

$$\begin{aligned} 0 = \ddot{z}_H &+ \frac{(Mr_H - 4M^2 - Q^2)z_H\dot{t}^2}{r_H^4} \\ &- \frac{[Mr_H^3 - 2M^2y_H^2 + Q^2(y_H^2 - z_H^2)]z_H\dot{z}_H^2}{r_H^6} \\ &- \frac{2My_H\dot{y}_H\dot{z}_H}{r_H^3} + \mathcal{O}(M^3). \end{aligned} \tag{A.6}$$

Here, $r_H = \sqrt{y_H^2 + z_H^2}$, a dot denotes the derivative with respect to ξ above, and $\dot{y}_H$ has been regarded to be of the order of M/b_P [90].

Similarly, we apply the iterative technique to the derivation of the gravitational deflection angle up to the 2PM order for light traveling in the polar-axis plane of the KN lens from the emitter $C(0,\ y_{CH},\ z_{CH})$ to the receiver $D(0,\ y_{DH},\ z_{DH})$, with $y_{CH} \approx -b_P$, $z_{CH} \ll -b_P$, and $z_{DH} \gg b_P$. By adopting the following boundary conditions

$$\dot{t}|_{\xi\to-\infty} = \dot{t}|_{z_H\to-\infty} = 1, \tag{A.7}$$

$$\dot{y}_H|_{\xi\to-\infty} = \dot{y}_H|_{z_H\to-\infty} = 0, \tag{A.8}$$

$$\dot{z}_H|_{\xi\to-\infty} = \dot{z}_H|_{z_H\to-\infty} = 1, \tag{A.9}$$

$$y_H|_{\xi\to-\infty} = y_H|_{z_H\to-\infty} = -b_P, \tag{A.10}$$

we can obtain the analytical expressions up to the 1PM order for $\dot{t}$, $\dot{y}_H$, $\dot{z}_H$, y_H, and the parameter transformation from equations (A.4)-(A.6)

$$\dot{t} = 1 + \frac{2M}{\sqrt{z_H^2 + b_P^2}} + \mathcal{O}(M^2), \tag{A.11}$$

$$\dot{y}_H = \frac{2Mz_H}{b_P\sqrt{z_H^2 + b_P^2}} + \mathcal{O}(M^2), \tag{A.12}$$

$$\dot{z}_H = 1 + \mathcal{O}(M^2), \tag{A.13}$$

$$y_H = -b_P\left(1 - \frac{2M\sqrt{z_H^2 + b_P^2}}{b_P^2}\right) + \mathcal{O}(M^2), \tag{A.14}$$

$$\mathrm{d}\xi = [1 + \mathcal{O}(M^2)]\mathrm{d}z_H. \tag{A.15}$$

Moreover, the substitution of equations (A.11)-(A.15) into the integration of equation (A.5) over ξ implies

$$\begin{aligned} \dot{y}_H = &\frac{2Mz_H}{b_P\sqrt{z_H^2 + b_P^2}} + \frac{M^2}{4b_P^2(z_H^2 + b_P^2)^2} \\ &\times \left[17b_P^3z_H + 15b_Pz_H^3 + 15(z_H^2 + b_P^2)^2\arctan\frac{z_H}{b_P}\right] \\ &- \frac{Q^2}{4b_P^2(z_H^2 + b_P^2)^2} \\ &\times \left[5b_P^3z_H + 3b_Pz_H^3 + 3(z_H^2 + b_P^2)^2\arctan\frac{z_H}{b_P}\right] \\ &+ \mathcal{O}(M^3). \end{aligned} \tag{A.16}$$

Subsequently, with the consideration of equations (A.13) and (A.16) and the conditions $z_{CH} \ll -b_P$ $(\approx y_{CH})$ and $z_{DH} \gg b_P$, the deflection angle up to the 2PM order of light in the polar-axis plane of a KN black hole takes the form in harmonic coordinates:

$$\begin{aligned} \alpha_P &= \arctan\frac{\dot{y}_H}{\dot{z}_H}\Big|_{z_H\to-\infty}^{z_H\to+\infty} = \frac{\dot{y}_H}{\dot{z}_H}\Big|_C^D + \mathcal{O}(M^3) \\ &= \frac{4M}{b_P} + \frac{15\pi M^2}{4b_P^2} - \frac{3\pi Q^2}{4b_P^2} + \mathcal{O}(M^3), \end{aligned} \tag{A.17}$$

which is the same as that given in (33) for the case of $v_3 = 0$.

ORCID iDs

Wenbin Lin https://orcid.org/0000-0002-4282-066X
Guansheng He https://orcid.org/0000-0002-6145-0449

References

[1] Refsdal S 1964 On the possibility of determining Hubble's parameter and the masses of galaxies from the gravitational lens effect *Mon. Not. R. Astron. Soc.* **128** 307
[2] Blandford R D and Narayan R 1992 Cosmological applications of gravitational lensing *Annu. Rev. Astron. Astrophys.* **30** 311
[3] Wambsganss J 1998 Gravitational lensing in astronomy *Living Rev. Relativ.* **1** 12
[4] Virbhadra K S and Ellis G F R 2000 Schwarzschild black hole lensing *Phys. Rev.* D **62** 084003
[5] Bozza V 2002 Gravitational lensing in the strong field limit *Phys. Rev.* D **66** 103001

[6] Keeton C R and Petters A O 2005 Formalism for testing theories of gravity using lensing by compact objects: Static, spherically symmetric case *Phys. Rev.* D **72** 104006

[7] Virbhadra K S 2009 Relativistic images of Schwarzschild black hole lensing *Phys. Rev.* D **79** 083004

[8] Reyes R, Mandelbaum R, Seljak U, Baldauf T, Gunn J E, Lombriser L and Smith R E 2010 Confirmation of general relativity on large scales from weak lensing and galaxy velocities *Nature* **464** 256

[9] Liu X *et al* 2016 Constraining $f(R)$ gravity theory using weak lensing peak statistics from the Canada-France-Hawaii-telescope lensing survey *Phys. Rev. Lett.* **117** 051101

[10] Zhao S-S and Xie Y 2016 Strong field gravitational lensing by a charged Galileon black hole *J. Cosmol. Astropart. Phys.* **2016** JCAP07(2016)007

[11] Liu X, Yang N and Jia J 2016 Gravitational lensing of massive particles in Schwarzschild gravity *Class. Quantum Grav.* **33** 175014

[12] Fan X-L, Liao K, Biesiada M, Piórkowska-Kurpas A and Zhu Z-H 2017 Speed of gravitational waves from strongly lensed gravitational waves and electromagnetic signals *Phys. Rev. Lett.* **118** 091102

[13] Zhao S-S and Xie Y 2017 Strong deflection gravitational lensing by a modified Hayward black hole *Eur. Phys. J.* C **77** 272

[14] Collett T E *et al* 2018 A precise extragalactic test of General Relativity *Science* **360** 1342

[15] Jusufi K, Övgün A, Saavedra J, Vásquez Y and González P A 2018 Deflection of light by rotating regular black holes using the Gauss–Bonnet theorem *Phys. Rev.* D **97** 124024

[16] Jung S and Shin C S 2019 Gravitational-wave fringes at LIGO: Detecting compact dark matter by gravitational lensing *Phys. Rev. Lett.* **122** 041103

[17] Lu X and Xie Y 2019 Weak and strong deflection gravitational lensing by a renormalization group improved Schwarzschild black hole *Eur. Phys. J.* C **79** 1016

[18] Marques G A, Liu J, Matilla J M Z, Haiman Z, Bernui A and Novaes C P 2019 Constraining neutrino mass with weak lensing Minkowski Functionals *J. Cosmol. Astropart. Phys.* **2019** JCAP06(2019)019

[19] Liu F-Y, Mai Y-F, Wu W-Y and Xie Y 2019 Probing a regular non-minimal Einstein–Yang–Mills black hole with gravitational lensings *Phys. Lett.* B **795** 475

[20] Zhu X-Y and Xie Y 2020 Strong deflection gravitational lensing by a Lee–Wick ultracompact object *Eur. Phys. J.* C **80** 444

[21] Chen Z, Luo W, Cai Y-F and Saridakis E N 2020 New test on general relativity and $f(T)$ torsional gravity from galaxy-galaxy weak lensing surveys *Phys. Rev.* D **102** 104044

[22] Mukherjee S, Wandelt B D and Silk J 2020 Multimessenger tests of gravity with weakly lensed gravitational waves *Phys. Rev.* D **101** 103509

[23] Lu X and Xie Y 2021 Gravitational lensing by a quantum deformed Schwarzschild black hole *Eur. Phys. J.* C **81** 627

[24] Gao Y-X and Xie Y 2021 Gravitational lensing by hairy black holes in Einstein-scalar-Gauss–Bonnet theories *Phys. Rev.* D **103** 043008

[25] Babar G Z, Atamurotov F and Babar A Z 2021 Gravitational lensing in 4-D Einstein–Gauss–Bonnet gravity in the presence of plasma *Phys. Dark Univ.* **32** 100798

[26] Cheng X-T and Xie Y 2021 Probing a black-bounce, traversable wormhole with weak deflection gravitational lensing *Phys. Rev.* D **103** 064040

[27] Zhang J and Xie Y 2022 Gravitational lensing by a black-bounce-Reissner–Nordström spacetime *Eur. Phys. J.* C **82** 471

[28] Gao Y-X and Xie Y 2022 Strong deflection gravitational lensing by an Einstein–Lovelock ultracompact object *Eur. Phys. J.* C **82** 162

[29] Liu X-H, Li Z-H, Qi J-Z and Zhang X 2022 Galaxy-scale test of general relativity with strong gravitational lensing *Astrophys. J.* **927** 28

[30] Javed W, Riaz S, Pantig R C and Övgün A 2022 Weak gravitational lensing in dark matter and plasma mediums for wormhole-like static aether solution *Eur. Phys. J.* C **82** 1057

[31] Virbhadra K S 2022 Distortions of images of Schwarzschild lensing *Phys. Rev.* D **106** 064038

[32] Soares A R, Pereira C F S, Vitória R L L and Rocha E M 2023 Holonomy corrected Schwarzschild black hole lensing *Phys. Rev.* D **108** 124024

[33] Soares A R, Vitória R L L and Pereira C F S 2023 Gravitational lensing in a topologically charged Eddington-inspired Born–Infeld spacetime *Eur. Phys. J.* C **83** 903

[34] Vachher A, Baboolal D and Ghosh S G 2024 Probing dark matter via strong gravitational lensing by black holes *Phys. Dark Univ.* **44** 101493

[35] Pahlavon Y, Atamurotov F, Jusufi K, Jamil M and Abdujabbarov A 2024 Effect of magnetized plasma on shadow and gravitational lensing of a Reissner–Nordström black hole *Phys. Dark Univ.* **45** 101543

[36] Hoshimov H, Yunusov O, Atamurotov F, Jamil M and Abdujabbarov A 2024 Weak gravitational lensing and shadow of a GUP-modified Schwarzschild black hole in the presence of plasma *Phys. Dark Univ.* **43** 101392

[37] Virbhadra K S 2024 Conservation of distortion of gravitationally lensed images *Phys. Rev.* D **109** 124004

[38] Birkinshaw M and Gull S F 1983 A test for transverse motions of clusters of galaxies *Nature* **302** 315

[39] Kopeikin S M and Schäfer G 1999 Lorentz covariant theory of light propagation in gravitational fields of arbitrary-moving bodies *Phys. Rev.* D **60** 124002

[40] Klioner S A and Peip M 2003 Numerical simulations of the light propagation in the gravitational field of moving bodies *Astron. Astrophys.* **410** 1063

[41] Wucknitz O and Sperhake U 2004 Deflection of light and particles by moving gravitational lenses *Phys. Rev.* D **69** 063001

[42] Heyrovský D 2005 Velocity effects on the deflection of light by gravitational microlenses *Astrophys. J.* **624** 28

[43] Kopeikin S M and Makarov V V 2007 Gravitational bending of light by planetary multipoles and its measurement with microarcsecond astronomical interferometers *Phys. Rev.* D **75** 062002

[44] Kopeikin S M and Fomalont E B 2007 Gravimagnetism, causality, and aberration of gravity in the gravitational light-ray deflection experiments *Gen. Relat. Gravit.* **39** 1583

[45] Deng X-M and Xie Y 2012 Two-post-Newtonian light propagation in the scalar-tensor theory: An N-point mass case *Phys. Rev.* D **86** 044007

[46] He G and Lin W 2014 Roto-translational effects on deflection of light and particle by moving Kerr black hole *Int. J. Mod. Phys.* D **23** 1450031

[47] Banik I and Zhao H 2015 Effects of lens motion and uneven magnification on image spectra *Mon. Not. R. Astron. Soc.* **450** 3155

[48] Deng X-M 2015 The second post-Newtonian light propagation and its astrometric measurement in the solar system *Int. J. Mod. Phys.* D **24** 1550056

[49] He G and Lin W 2016 Gravitational deflection of light and massive particles by a moving Kerr–Newman black hole *Class. Quantum Grav.* **33** 095007

[50] He G and Lin W 2017 Analytical derivation of second-order deflection in the equatorial plane of a radially moving Kerr–Newman black hole *Class. Quantum Grav.* **34** 105006

[51] Zschocke S 2018 Light propagation in 2PN approximation in the field of one moving monopole I. Initial value problem *Class. Quantum Grav.* **35** 055013

[52] Zschocke S 2019 Light propagation in 2PN approximation in the field of one moving monopole II. Boundary value problem *Class. Quantum Grav.* **36** 015007

[53] Li W, Feng Z, Zhou X, Mu X and He G 2021 Kerr–Schild form of the exact metric for a constantly moving Kerr black hole and null gravitational deflection *Int. J. Mod. Phys.* D **30** 2150067

[54] Pyne T and Birkinshaw M 1993 Null geodesics in perturbed spacetimes *Astrophys. J.* **415** 459

[55] Cordes J M, Romani R W and Lundgren S C 1993 The Guitar nebula: a bow shock from a slow-spin, high-velocity neutron star *Nature* **362** 133

[56] Chatterjee S, Vlemmings W H T, Brisken W F, Lazio T J W, Cordes J M, Goss W M, Thorsett S E, Fomalont E B, Lyne A G and Kramer M 2005 Getting its kicks: A VLBA parallax for the hyperfast pulsar B1508+55 *Astrophys. J. Lett.* **630** L61

[57] Perryman M A C *et al* 2001 GAIA: Composition, formation and evolution of the Galaxy *Astron. Astrophys.* **369** 339

[58] Prusti T *et al* 2016 The Gaia mission *Astron. Astrophys.* **595** A1

[59] Shao M and Nemati B 2009 Sub-microarcsecond astrometry with sim-lite: a testbed-based performance assessment *Publ. Astron. Soc. Pac.* **121** 41

[60] Reid M J *et al* 2009 Trigonometric parallaxes of massive star-forming regions. VI. galactic structure, fundamental parameters, and noncircular motions *Astrophys. J.* **700** 137

[61] Chen D 2014 STEP mission: high-precision space astrometry to search for terrestrial exoplanets *J. Instrum.* **9** C04040

[62] Malbet F *et al* 2012 High precision astrometry mission for the detection and characterization of nearby habitable planetary systems with the Nearby Earth Astrometric Telescope (NEAT) *Exp. Astron.* **34** 385

[63] Reid M J and Honma M 2014 Microarcsecond radio astrometry *Ann. Rev. Astron. Astrophys.* **52** 339

[64] Malbet F, Crouzier A, Léger A, Shao M and Goullioud R 2014 NEAT: ultra-precise differential astrometry to characterize planetary systems with Earth-mass exoplanets in the vicinity of our Sun *Proc. SPIE* **9143** 91432L

[65] Trippe S, Davies R, Eisenhauer F, Schreiber N. M. Förster, Fritz T K and Genzel R 2010 High-precision astrometry with MICADO at the European extremely large telescope *Mon. Not. R. Astron. Soc.* **402** 1126

[66] Zhang B, Reid M J, Menten K M, Zheng X W, Brunthaler A, Dame T M and Xu Y 2013 Parallaxes for W49N and G048.60+0.02: distant star forming regions in the perseus spiral arm *Astrophys. J.* **775** 79

[67] Murphy E J *et al* 2018 The ngVLA science case and associated science requirements *Science with a Next Generation Very Large Array ASP Conf. Series* Vol. 517, 3 arXiv:1810.07524

[68] Rioja M J and Dodson R 2020 Precise radio astrometry and new developments for the next-generation of instruments *Astron. Astrophys. Rev.* **28** 6

[69] Brown A G A 2021 Microarcsecond astrometry: science highlights from Gaia *Ann. Rev. Astron. Astrophys.* **59** 59

[70] Li Y, Xu Y, Li J, Wu Y, Bian S, Lin Z, Yang W, Hao C and Liu D 2022 Light deflection under the gravitational field of Jupiter-testing General Relativity *Astrophys. J.* **925** 47

[71] Li Y, Xu Y, Bian S, Lin Z, Li J, Liu D and Hao C 2022 The effect of light deflection by solar system objects on high-precision square kilometre array astrometry *Astrophys. J.* **938** 58

[72] Braun R, Bourke T, Green J A, Keane E and Wagg J 2015 Advancing astrophysics with the square kilometre array *Proc. Sci.* **AASKA14** 174

[73] Baker T and Trodden M 2017 Multimessenger time delays from lensed gravitational waves *Phys. Rev.* D **95** 063512

[74] Mészáros P, Fox D B, Hanna C and Murase K 2019 Multi-messenger astrophysics *Nat. Rev. Phys.* **1** 585

[75] (IceCube Collaboration) *et al* 2018 Multimessenger observations of a flaring blazar coincident with high-energy neutrino IceCube-170922A *Science* **361** eaat1378

[76] Qi J-Z, Jin S-J, Fan X-L, Zhang J-F and Zhang X 2021 Using a multi-messenger and multi-wavelength observational strategy to probe the nature of dark energy through direct measurements of cosmic expansion history *J. Cosmol. Astropart. Phys.* **2021** JCAP12(2021)042

[77] He G, Xie Y, Jiang C and Lin W 2024 Gravitational lensing of massive particles by a black-bounce-Schwarzschild black hole *Phys. Rev.* D **110** 064008

[78] Sereno M and de Luca F 2006 Analytical Kerr black hole lensing in the weak deflection limit *Phys. Rev.* D **74** 123009

[79] Gyulchev G N and Yazadjiev S S 2010 Analytical Kerr–Sen dilaton-axion black hole lensing in the weak deflection limit *Phys. Rev.* D **81** 023005

[80] Aazami A B, Keeton C R and Petters A O 2011 Lensing by Kerr black holes. II: Analytical study of quasi-equatorial lensing observables *J. Math. Phys.* **52** 102501

[81] Jiang T, Xu X and Jia J 2023 Off-equatorial deflections and gravitational lensing. I. In Kerr spacetime and effect of spin arXiv:2307.15174

[82] Klioner S A 2003 Light propagation in the gravitational field of moving bodies by means of Lorentz transformation I. Mass monopoles moving with constant velocities *Astron. Astrophys.* **404** 783

[83] He G-S and Lin W-B 2014 Exact harmonic metric for a uniformly moving Schwarzschild black hole *Commun. Theor. Phys.* **61** 270

[84] He G-S and Lin W-B 2014 The exact harmonic metric for a moving Reissner–Nordström black hole *Chin. Phys. Lett.* **31** 090401

[85] Debney G C, Kerr R P and Schild A 1969 Solutions of the Einstein and Einstein–Maxwell Equations *J. Math. Phys.* **10** 1842

[86] Aguirregabiria J M, Chamorro A and Virbhadra K S 1996 Energy and angular momentum of charged rotating black holes *Gen. Relat. Gravit.* **28** 1393

[87] Xulu S S 2000 Møller energy for the Kerr–Newman Metric *Mod. Phys. Lett.* A **15** 1511

[88] Newman E and Adamo T 2014 Kerr–Newman metric *Scholarpedia* **9** 31791

[89] Weinberg S 1972 *Gravitation and Cosmology: Principles and Applications of the General Theory of Relativity* (New York: Wiley)

[90] He G and Lin W 2016 Second-order time delay by a radially moving Kerr–Newman black hole *Phys. Rev.* D **94** 063011

[91] González J A, Sperhake U, Brügmann B, Hannam M and Husa S 2007 Maximum Kick from Nonspinning Black-Hole Binary Inspiral *Phys. Rev. Lett.* **98** 091101

[92] Bland-Hawthorn J and Gerhard O 2016 The galaxy in context: structural, kinematic, and integrated properties *Annu. Rev. Astron. Astrophys.* **54** 529

[93] Parsa M, Eckart A, Shahzamanian B, Karas V, Zajaček M, Zensus J A and Straubmeier C 2017 Investigating the relativistic motion of the stars near the supermassive black hole in the galactic center *Astrophys. J.* **845** 22

[94] He G, Zhou X, Feng Z, Mu X, Wang H, Li W, Pan C and Lin W 2020 Gravitational deflection of massive particles in Schwarzschild–de Sitter spacetime *Eur. Phys. J.* C **80** 835

[95] Abuter R *et al* 2017 First light for GRAVITY: Phase referencing optical interferometry for the Very Large Telescope Interferometer *Astron. Astrophys.* **602** A94